

# Viscosity of Gaseous Mixtures of HFC-125 + HFC-32<sup>1</sup>

C. Yokoyama,<sup>2, 3</sup> T. Nishino,<sup>2</sup> and M. Takahashi<sup>2</sup>

---

This paper reports experimental results for the viscosity of gaseous mixtures of HFC-125 (pentafluoroethane) + HFC-32 (difluoromethane). The measurements were carried out with an oscillating-disk viscometer of the Maxwell type at temperatures from 298.15 to 423.15 K. The viscosity was measured for three mixtures (mole fraction of HFC-125 is 0.7498, 0.4998, or 0.2475). The viscosity at normal pressure was analyzed with the extended law of corresponding states developed by Kestin et al. and the scaling parameters were obtained for unlike-pair interactions between HFC-125 and HFC-32. The modified Enskog theory developed by Vesovic and Wakeham was applied to predict the viscosity for the binary gaseous mixtures under pressure. For the calculation of the pseudo-radial distribution function in mixtures, a method based on the Carnahan–Starling equation for the radial distribution function of hard sphere mixtures is proposed.

---

**KEY WORDS:** corresponding states; Enskog theory; HFC-125; HFC-32; mixture model; viscosity.

## 1. INTRODUCTION

Chlorofluorocarbons (CFCs) and hydrochlorofluorocarbons (HCFCs) must be completely phased out in the near-future. The potential alternatives proposed are hydrofluorocarbons (HFCs), such as HFC-125 (pentafluoroethane), HFC-134a (1,1,1,2-tetrafluoroethane), HFC-143a (1,1,1-trifluoroethane), and HFC-32 (difluoromethane), and their binary and/or ternary mixtures.

Transport properties, such as viscosity, of the alternative refrigerants influence the economical feasibility of heat exchangers, which can come

---

<sup>1</sup> Paper presented at the Fourteenth Symposium on Thermophysical Properties, June 25–30, 2000, Boulder, Colorado, U.S.A.

<sup>2</sup> Institute for Chemical Reaction Science, Tohoku University, Katahira 2-1-1, Sendai 980-8577, Japan.

<sup>3</sup> To whom correspondence should be addressed. E-mail: chiaki@tagen.tohoku.ac.jp

close to the theoretical efficiency of the thermodynamic cycle with CFCs. Therefore, reliable prediction methods for the transport properties of mixed HFCs are required to establish the process design methodology for a search of the optimum operation conditions of the refrigeration systems with the use of HFCs.

In our previous studies, we measured the gaseous viscosity of HFC-32, HFC-134a, HFC-143a, HFC-125 [1–4], and the HFC-125+HFC-134a system [5]. As part of a continuing study of the viscosity of dense fluid systems containing HFCs, measurements of the viscosity of gaseous mixtures of HFC-125+HFC-32, made between 298.15 and 423.15 K at pressures up to 6.6 MPa, are reported here. The viscosity data at 0.1 MPa were used to determine the scaling parameters of the unlike-pair interactions between HFC-125 and HFC-32 from the extended law of corresponding states [6]. The viscosity data under pressure were analyzed with the extended Enskog theory developed by Vesovic and Wakeham [7]. We propose a newly developed method to determine the pseudo-radial distribution function for species  $i$  and  $j$  in the mixtures.

## 2. EXPERIMENTAL

The viscosity was measured with an oscillating-disk viscometer of the Maxwell type. The gas density under the experimental conditions of the viscosity measurement was measured with a high-pressure gas pipette. The experimental apparatus and procedures were the same as those described in previous studies [8–10]. The apparatus constant of the viscometer under the experimental temperature and pressure conditions was determined by considering the viscosity data of nitrogen taken from Stephan et al. [11] and the nitrogen gas density data from Jacobsen et al. [12]. As for the gas density determination, the second virial coefficient data for the HFC-125+HFC-32 binary gas mixture reported by Weber [13, 14] were used to determine the gas compressibility factor values under expanded conditions in a glass cylinder in the gas density measurement apparatus [8, 9]. The samples were prepared in a sample vessel by charging first the less volatile constituent gas (HFC-125) and then the more volatile one (HFC-32). When the sample gas mixture was loaded into the viscometer vessel, the temperature of the sample vessel and the connecting tubing between the sample vessel and the viscometer vessel were thermostated at about 423 K to prevent condensation.

The temperature of the thermostat was measured with a quartz thermometer calibrated against a Leed–Northrup platinum resistance thermometer and was kept constant to about 0.003 K over the period of the measurements. The temperature of the viscometer was maintained to

within 0.001 K. The pressure of the sample was measured with a mercury U-tube detector and a deadweight gauge. Temperature and pressure values have an uncertainty of 0.01 K and 0.5 kPa, respectively. The density was measured with the high-pressure gas pipette and low-pressure gas expansion system. An inner space of the gas pipette was kept at the same level as that of the oscillating disk in the viscometer. This configuration of the oscillating disk and gas pipette was adopted from a density distribution due to gravity force near the critical point. Density values have an uncertainty of  $0.05 \text{ kg} \cdot \text{m}^{-3}$ . It should be noted that the uncertainty of the density measurements is determined mainly from the compressibility value of the gas mixture sample expanded to about 0.1 MPa and 298.15 K. The details of the gas pipette and density determination were described by Takahashi et al. [9]. The compositions of the sample mixtures were determined by weighing. The uncertainty of the composition determination was estimated to be less than  $10^{-4}$  mole fraction. The accuracy of the present viscosity measurements was estimated to be 0.4% considering the uncertainties in the determination of the logarithmic decrement, the period of oscillation, the density of the gas, the composition of the gas mixture, and other sources of error.

The HFC-125 and HFC-32 samples were supplied by Asahi Glass Co. Ltd. The purity of both samples, certified by the suppliers, was approximately 99.9 mol%. The samples were further purified by distillation several times before preparing mixture samples.

### 3. RESULTS AND DISCUSSION

The experimental results for the viscosity and density of the HFC-125 + HFC-32 system are presented in Table I. The viscosity values of the mixture of HFC-125 (0.4998) + HFC-134a (0.5002) are shown in Figs. 1 and 2. As shown in Fig. 1, the curves as a function of pressure intersect for the isotherms from 348.15 to 423.15 K, but the curves as a function of density do not, as shown in Fig. 2. Similar behavior was observed in the other two mixtures and also for the pure HFCs and HFC-125 + HFC-134a binary systems studied previously [1–5].

The viscosity of gaseous mixtures at 0.1 MPa,  $\eta_0$ , are plotted as a function of mole fraction in Fig. 3, in which the viscosities of HFC-125 [4] and HFC-32 [1] are also shown. As shown in Fig. 3, the shape of the curves for  $\eta_0$  is slightly convex upward in the present experimental temperature range. This behavior is typical for the viscosity of gaseous mixtures at 0.1 MPa.

The extended law of corresponding states for the transport properties was applied to determine the scaling parameters for the binary interaction

**Table I.** Experimental Viscosity for the HFC-125 + HFC-32 System  
 ( $x_{\text{HFC-125}}$  is the Mole Fraction of HFC-125)

$T$ (K)	$P$ (MPa)	$\rho$ ( $\text{kg} \cdot \text{m}^{-3}$ )	$\eta$ ( $\mu\text{Pa} \cdot \text{s}$ )	
$x_{\text{HFC-125}} = 0.7498$				
298.15	0.1033	4.349	13.093	
	0.2271	9.750	13.073	
	0.3684	16.092	13.063	
	0.4892	21.922	13.051	
	0.5863	26.732	13.051	
	0.7188	33.613	13.050	
	0.8694	41.966	13.086	
	1.0004	49.791	13.114	
	1.1236	57.747	13.198	
	1.3443	73.263	13.294	
	323.15	0.1021	3.956	14.064
		0.2460	9.683	14.110
		0.3906	15.634	14.096
		0.5377	21.913	14.100
0.6827		28.350	14.139	
0.8280		35.069	14.177	
0.9765		42.139	14.176	
1.1210		49.352	14.252	
1.2665		56.946	14.325	
1.4261		65.684	14.409	
1.5619		73.932	14.502	
1.7123		83.194	14.605	
1.8563		92.724	14.716	
2.0028		103.81	14.894	
2.2154	120.83	15.152		
2.3364	132.09	15.337		
2.4833	147.31	15.647		
348.15	0.1028	3.688	15.157	
	0.2898	10.561	15.140	
	0.4906	18.199	15.166	
	0.6823	25.769	15.222	
	0.9277	35.899	15.265	
	1.1713	46.220	15.345	
	1.4148	57.296	15.451	
	1.6701	69.581	15.597	
	1.9011	81.449	15.755	
	2.1514	94.856	15.977	
	2.4120	110.46	16.216	
	2.6578	126.57	16.540	
	2.8920	143.35	16.865	
	3.1943	167.59	17.435	
3.4517	192.04	18.045		

Table I. (Continued)

$T$ (K)	$P$ (MPa)	$\rho$ ( $\text{kg} \cdot \text{m}^{-3}$ )	$\eta$ ( $\mu\text{Pa} \cdot \text{s}$ )
373.15	3.7574	227.31	19.048
	4.0379	269.78	20.471
	4.2491	313.68	22.151
	0.1026	3.430	16.093
	0.3831	13.038	16.168
	0.6707	23.289	16.173
	0.9512	33.718	16.295
	1.2366	44.833	16.412
	1.5198	55.969	16.515
	1.8158	68.558	16.705
	2.1451	82.979	16.913
	2.4423	97.037	17.161
	2.7126	110.59	17.381
	3.0417	127.97	17.745
	3.3230	144.17	18.061
	3.5839	160.13	18.449
	3.8295	176.40	18.893
	4.0899	194.34	19.363
	4.3834	217.22	20.065
	4.5949	234.64	20.600
398.15	4.8513	257.52	21.354
	5.0590	279.05	22.128
	5.2713	301.48	22.966
	0.1015	3.173	17.113
	0.4385	13.950	17.185
	0.7835	25.371	17.224
	1.1196	36.415	17.384
	1.4667	49.215	17.526
	1.8622	63.986	17.675
	2.1801	76.205	17.844
	2.5538	91.223	18.108
	2.8222	102.64	18.316
	3.1684	117.93	18.651
	3.4644	131.77	18.898
	3.7677	146.42	19.285
	4.0838	162.22	19.674
	4.4104	179.33	20.138
	4.7032	195.85	20.583
	4.9995	213.12	21.105
	5.2832	230.86	21.623
5.5482	248.01	22.218	
5.8797	270.34	23.045	
6.1089	286.73	23.721	
423.15	0.1026	3.006	18.016
	0.3871	11.511	18.097

Table I. (Continued)

$T$ (K)	$P$ (MPa)	$\rho$ (kg·m <sup>-3</sup> )	$\eta$ ( $\mu$ Pa·s)
	0.6820	20.538	18.144
	1.0195	31.158	18.250
	1.4116	43.932	18.351
	1.8097	57.012	18.572
	2.1813	69.700	18.737
	2.4719	80.052	18.932
	2.7225	89.117	19.039
	3.0801	102.42	19.330
	3.3882	114.28	19.564
	3.6927	126.33	19.839
	3.9808	138.19	20.073
	4.2443	151.32	20.418
	4.6056	165.01	20.825
	4.9136	178.95	21.124
	5.2529	194.60	21.618
	5.5211	207.39	21.992
	5.8390	222.90	22.466
	6.1025	236.39	22.972
	6.4329	253.47	23.529
	6.8112	273.66	24.218
	7.1132	290.18	24.905
	7.4111	306.89	25.535
	$x_{\text{HFC-125}} = 0.4998$		
298.15	0.1015	3.568	13.057
	0.1978	7.046	12.981
	0.3468	12.620	12.991
	0.4936	18.373	12.984
	0.6397	24.396	12.992
	0.7819	30.753	12.996
	0.9278	37.595	13.023
	1.0748	44.824	13.053
	1.2311	53.079	13.069
	1.3799	61.836	13.139
323.15	0.1018	3.291	14.093
	0.2958	9.752	14.066
	0.4898	16.495	14.080
	0.6841	23.565	14.092
	0.8796	31.046	14.113
	1.0797	39.147	14.152
	1.2707	47.208	14.194
	1.4687	56.164	14.263
	1.6762	66.168	14.369
	1.8567	75.610	14.479
	2.0678	87.939	14.609
	2.2032	96.252	14.735

Table I. (Continued)

$T$ (K)	$P$ (MPa)	$\rho$ (kg·m <sup>-3</sup> )	$\eta$ ( $\mu$ Pa·s)
348.15	2.3439	105.80	14.886
	2.5003	117.51	15.075
	0.1011	3.028	15.150
	0.1013	3.031	15.155
	0.4009	12.283	15.169
	0.7115	22.380	15.225
	1.0162	32.866	15.281
	1.3257	44.177	15.364
	1.6057	54.815	15.470
	1.9352	68.454	15.620
	2.2757	83.837	15.834
	2.5173	95.523	15.996
	2.7272	107.05	16.188
	2.9301	117.83	16.438
	3.1883	133.84	16.774
	3.4038	148.49	17.073
	3.6231	165.08	17.482
	3.8501	184.21	18.003
	4.0520	204.99	18.554
	373.15	4.2104	223.42
4.3256		238.84	19.685
4.4789		262.96	20.517
4.5844		283.44	21.340
0.1021		2.848	16.231
0.3485		9.861	16.275
0.5945		16.927	16.320
0.9066		26.596	16.360
1.2179		36.436	16.445
1.5324		46.856	16.546
1.8384		57.363	16.675
2.1432		68.560	16.828
2.5136		82.782	17.052
2.8252		95.469	17.253
3.1902		111.44	17.586
3.4674		124.33	17.781
3.8625		144.06	18.297
4.1785		161.74	18.742
4.4256		176.45	19.094
4.6983		194.28	19.613
4.9317	210.15	20.139	
5.2083	230.90	20.780	
5.4675	252.45	21.563	
5.7579	279.07	22.527	
5.9959	303.41	23.465	
6.2043	327.28	24.462	
6.3614	345.03	25.322	

Table I. (Continued)

$T$ (K)	$P$ (MPa)	$\rho$ ( $\text{kg} \cdot \text{m}^{-3}$ )	$\eta$ ( $\mu\text{Pa} \cdot \text{s}$ )
398.15	0.1018	2.658	17.275
	0.4106	10.874	17.305
	0.7564	20.369	17.381
	1.0879	29.800	17.480
	1.4116	39.347	17.541
	1.6916	47.912	17.640
	2.3044	67.809	17.903
	2.6481	79.793	18.097
	2.7329	82.854	18.154
	3.0372	92.257	18.361
	3.3691	104.34	18.581
	3.6685	116.02	18.860
	4.0250	130.31	19.131
	4.3743	145.16	19.472
	4.6942	159.28	19.901
	5.1529	181.07	20.515
	5.4597	196.29	20.952
	5.7776	213.22	21.464
	6.1243	231.99	22.084
	6.4572	251.85	22.774
6.7770	271.53	23.480	
7.0381	288.55	24.157	
423.15	0.1015	2.490	18.346
	0.3432	8.416	18.430
	0.5835	14.575	18.453
	0.8777	22.174	18.527
	1.2583	32.282	18.626
	1.5547	40.387	18.709
	1.8254	47.984	18.811
	2.1330	56.862	18.930
	2.4385	66.196	19.072
	2.8285	78.376	19.242
	3.1177	87.898	19.423
	3.4579	99.369	19.660
	3.7682	106.97	19.917
	4.0878	117.68	20.134
	4.3634	127.22	20.343
	4.6771	138.80	20.611
	4.9609	148.97	20.845
	5.2206	158.61	21.112
	5.5227	170.56	21.405
	5.8070	181.72	21.784
6.0780	192.73	22.117	
6.3841	205.30	22.516	
6.7408	220.08	23.045	
7.0130	232.67	23.419	



Table I. (Continued)

$T$ (K)	$P$ (MPa)	$\rho$ ( $\text{kg} \cdot \text{m}^{-3}$ )	$\eta$ ( $\mu\text{Pa} \cdot \text{s}$ )
$x_{\text{HFC-125}} = 0.2475$			
298.15	0.1012	2.856	12.914
	0.2255	6.445	12.855
	0.3741	10.912	12.846
	0.4925	14.618	12.842
	0.6456	19.620	12.809
	0.7919	24.663	12.833
	0.9304	30.225	12.805
	1.0823	36.040	12.799
	1.2358	42.486	12.858
	1.3637	48.208	12.852
	323.15	0.1013	2.620
0.2925		7.704	13.999
0.4879		13.110	13.974
0.6784		18.606	13.979
0.9010		25.361	13.999
1.1231		32.512	14.016
1.3094		38.795	14.044
1.4691		44.556	14.064
1.6396		50.924	14.130
1.9684		64.349	14.240
2.1371		72.037	14.333
2.2682		78.372	14.402
2.4382		87.380	14.541
2.5998		96.654	14.677
348.15	2.7081	103.49	14.769
	0.1020	2.443	15.059
	0.3010	7.315	15.017
	0.4958	12.288	15.029
	0.6933	17.365	15.036
	0.8994	22.917	15.051
	1.1207	29.117	15.102
	1.3405	35.540	15.147
	1.5646	42.277	15.204
	1.7656	48.602	15.229
	1.9503	54.711	15.314
	2.1869	62.889	15.404
	2.3697	69.454	15.488
	2.5714	77.050	15.601
	2.7443	84.104	15.687
2.9469	92.724	15.839	
3.2165	105.26	16.046	
3.4231	115.55	16.282	
3.6220	126.31	16.542	

Table I. (Continued)

$T$ (K)	$P$ (MPa)	$\rho$ (kg·m <sup>-3</sup> )	$\eta$ ( $\mu$ Pa·s)
373.15	3.8239	138.50	16.732
	4.0105	150.64	17.048
	4.2194	166.29	17.454
	4.4608	187.30	18.103
	4.6069	202.64	18.540
	4.8006	221.45	19.431
	0.1010	2.263	16.125
	0.2897	6.532	16.124
	0.4870	11.106	16.123
	0.6837	15.774	16.157
	0.9279	21.736	16.189
	1.1694	27.826	16.249
	1.4166	34.189	16.285
	1.6655	40.906	16.334
	1.9098	47.703	16.425
	2.1515	54.633	16.509
	2.4068	62.182	16.608
	2.6395	69.494	16.734
	2.8869	77.470	16.850
	3.1850	87.565	17.013
	3.4382	96.604	17.181
	3.6556	105.17	17.345
	3.8694	113.13	17.484
	4.1507	124.68	17.816
	4.4407	137.86	18.107
	4.6753	148.99	18.399
	4.8597	158.39	18.641
5.1239	172.00	19.043	
5.3158	183.26	19.430	
5.5278	196.17	19.789	
5.7789	213.45	20.382	
5.9879	228.19	20.889	
6.1579	241.47	21.420	
6.3636	258.43	22.096	
6.5311	273.39	22.726	
6.7264	292.34	23.521	
6.8884	309.39	24.329	
6.9884	324.13	24.858	
398.15	0.1015	2.119	17.181
	0.3715	7.852	17.250
	0.6626	14.191	17.270
	0.9476	20.571	17.328
	1.2239	26.935	17.373
	1.5278	34.052	17.412
	1.8243	41.213	17.516
	2.1660	49.767	17.651

Table I. (Continued)

$T$ (K)	$P$ (MPa)	$\rho$ ( $\text{kg} \cdot \text{m}^{-3}$ )	$\eta$ ( $\mu\text{Pa} \cdot \text{s}$ )
423.15	2.4391	56.886	17.682
	2.7233	64.467	17.842
	3.0300	72.919	17.975
	3.3768	82.801	18.163
	3.7013	92.673	18.336
	4.0016	102.00	18.515
	4.2940	111.43	18.749
	4.6289	122.96	18.972
	4.9136	133.14	19.230
	5.1899	143.31	19.492
	5.4971	155.24	19.844
	5.7874	166.93	20.192
	6.0235	177.12	20.478
	6.2584	187.14	20.822
	6.5085	198.57	21.187
	6.7783	211.37	21.636
	7.0231	223.77	22.065
	7.2564	235.10	22.460
	0.1018	1.999	18.268
	0.2910	5.751	18.298
	0.4896	9.746	18.307
	0.7802	15.694	18.327
	1.0668	21.692	18.398
	1.3617	28.006	18.433
	1.6553	34.446	18.510
	1.9441	40.720	18.604
	2.2611	47.930	18.659
	2.5568	54.688	18.770
	2.8355	62.201	18.844
	3.1914	70.063	19.006
	3.4575	76.901	19.156
	3.7506	84.314	19.313
	4.0859	93.237	19.444
	4.3958	101.89	19.642
	4.6695	109.44	19.846
	5.0060	119.07	20.075
	5.2855	127.41	20.251
	5.5514	135.51	20.498
	5.8943	146.29	20.777
	6.2655	158.17	21.104
6.6209	170.14	21.484	
6.9002	180.04	21.753	
7.2113	191.16	22.228	
7.5099	202.01	22.498	
7.7205	210.30	22.831	

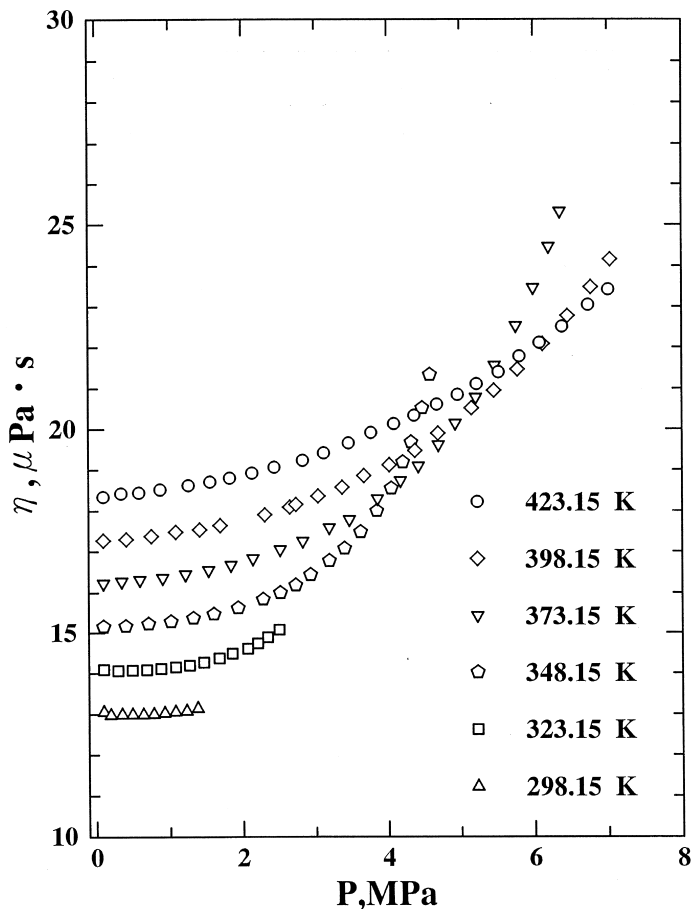


Fig. 1. Viscosity of the binary gaseous mixture of HFC-125 (0.4998)+ HFC-32 (0.5002) as a function of pressure.

between HFC-125 and HFC-32. The equations used are the same as given by Kestin et al. [6]. The scaling parameters of HFC-125 and HFC-32 are determined from least-squares fitting to the viscosity data for each of the pure HFCs reported previously [1, 4]. The optimum values of the scaling parameters between the HFC-125 and the HFC-32 pair interaction were determined using the viscosity data measured in this study. The values of the scaling parameters obtained are listed in Table II. The results calculated with the parameters in Table II are shown as the solid lines in Fig. 3. The average deviation between the experimental viscosity results and the calculated values is 0.29%, and the maximum deviation is 0.86%.

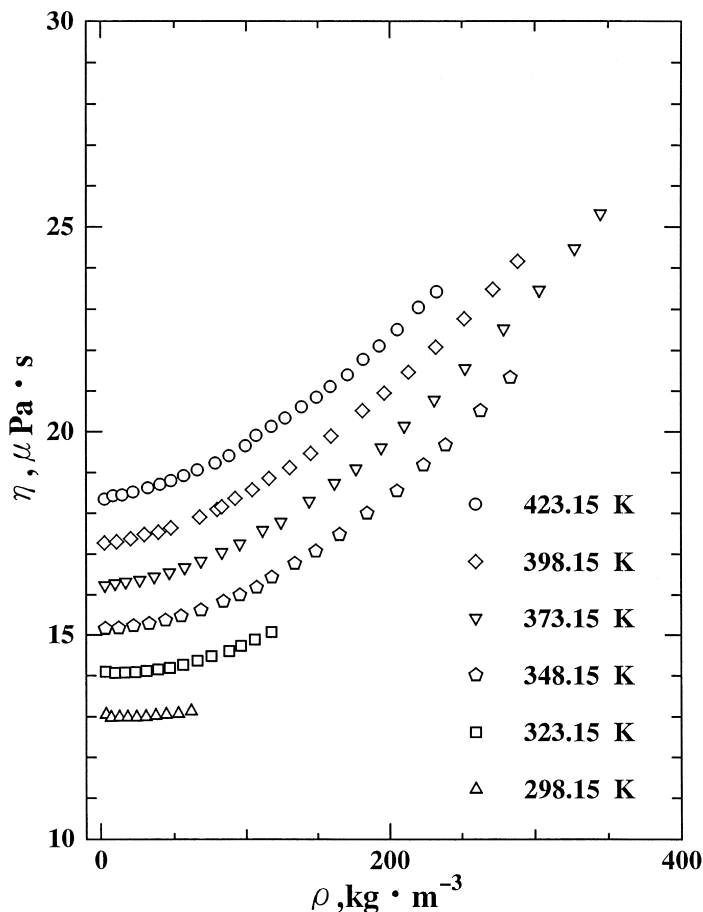


Fig. 2. Viscosity of the binary gaseous mixture of HFC-125 (0.4998)+ HFC-32 (0.5002) as a function of density.

The viscosity under pressure was analyzed with the extended Enskog theory developed by Vesovic and Wakeham (V-W method) [7]. In the V-W method, we need the equations for the viscosity of the pure constituent gases at 0.1 MPa and under pressure and for the mixture at 0.1 MPa. The viscosities at 0.1 MPa are obtained from the extended law of corresponding states described above. The viscosities of pure HFC-125 and HFC-32 are calculated with a residual viscosity equation expressed as follows:

$$\eta - \eta_0 = a_1(\rho - \rho_0) + a_2(\rho - \rho_0)^2 + a_3(\rho - \rho_0)^3 \quad (1)$$

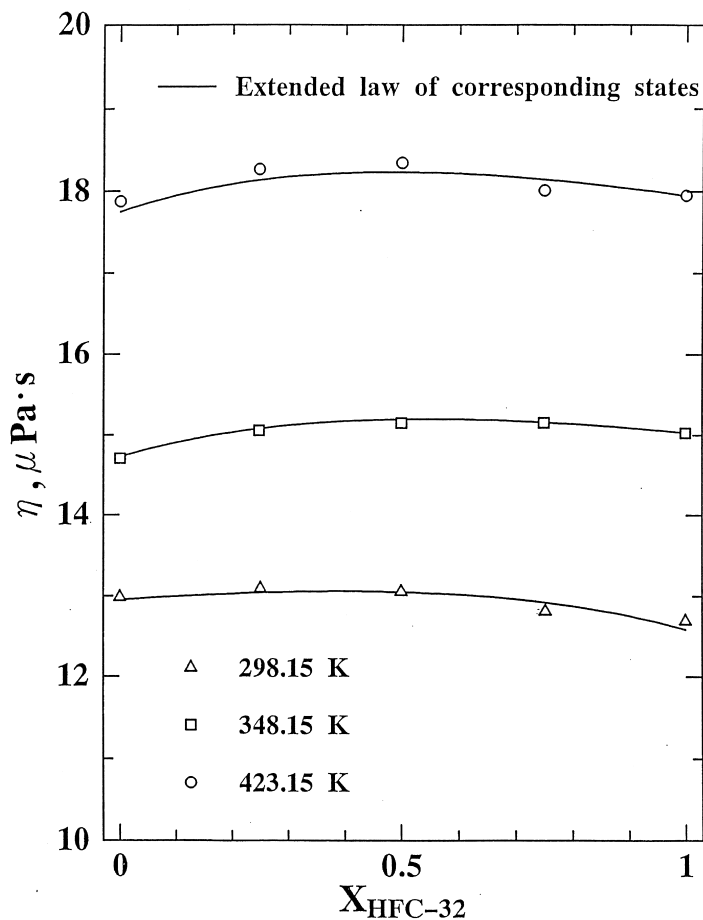


Fig. 3. Viscosity of the binary gaseous mixture of HFC-125 (0.4998)+ HFC-32 (0.5002) at 0.1 MPa.

Table II. Scaling Parameters for HFC-125 and HFC-32

$i-j$	$\varepsilon/k$ (K)	$\sigma$ (nm)
HFC-125-HFC-125	235.85	0.52600
HFC-32-HFC-32	277.46	0.41530
HFC-125-HFC-32	265.25	0.46024

and

$$a_1 = a_{10}T + a_{11} + a_{12}/T \quad (2)$$

$$a_2 = a_{20}T + a_{21} + a_{22}/T \quad (3)$$

$$a_3 = a_{30} + a_{31}/T + a_{32}/T^2 \quad (4)$$

where  $\eta$  is the viscosity under pressure in  $\mu\text{Pa}\cdot\text{s}$ ,  $\eta_0$  is the gas viscosity at 0.1 MPa in  $\mu\text{Pa}\cdot\text{s}$ ,  $\rho$  is the gas density under pressure in  $\text{kg}\cdot\text{m}^{-3}$ ,  $\rho_0$  is the gas density at 0.1 MPa in  $\text{kg}\cdot\text{m}^{-3}$ ,  $T$  is the absolute temperature in K, and the  $a_{ij}$  are parameters. The values of  $a_{ij}$  for HFC-125 and HFC-32 are listed in Table III. While Eqs. (1)–(4) represent the experimental viscosity values with absolute average deviations less than 0.20% for HFC-125 and 0.30% for HFC-32 in our experimental region, it should not be used at temperatures and/or densities outside of our experimental conditions. In the V-W method, the mean free path shorting factor,  $\alpha_{ii}$ , and the switch-over density are obtained from the following relation:

$$(d\eta_i/d\rho)|_T = \eta_i/\rho \quad (5)$$

In the lower-temperature range, below 348.15 K, the switch-over densities at which Eq. (5) holds are much higher than the maximum density under the present experimental conditions. Therefore, Eqs. (1)–(4) should not be applicable to Eq. (5). Thus the Lee–Thodos (LT) viscosity correlation [15] was applied to Eq. (5). In the LT correlation, we used the extended law of corresponding states to calculate the viscosity at 0.1 MPa and treated the triple point temperature as the adjustable parameter to improve the agreement between the experimental viscosity and the

Table III. Constants in Eqs. (1)–(4)

	HFC-125	HFC-32
$a_{10}$	$-8.736826 \times 10^{-5}$	$1.581357 \times 10^{-5}$
$a_{11}$	$8.042472 \times 10^{-2}$	$3.667580 \times 10^{-2}$
$a_{12}$	$-1.56065 \times 10$	$-1.511928 \times 10$
$a_{20}$	$-3.957473 \times 10^{-7}$	$2.629959 \times 10^{-6}$
$a_{21}$	$4.434098 \times 10^{-4}$	$-2.049982 \times 10^{-3}$
$a_{22}$	$-9.014753 \times 10^{-2}$	$4.362916 \times 10^{-1}$
$a_{30}$	$4.536891 \times 10^7$	$-2.413426 \times 10^{-6}$
$a_{31}$	$-4.307842 \times 10^{-4}$	$1.236867 \times 10^{-8}$
$a_{32}$	$9.75525 \times 10^{-2}$	$-1.602793 \times 10^{-11}$

correlated values. The optimum value of the triple-point temperature was 144.88 K for HFC-125 and 162.06 K for HFC-32.

For the mixture viscosity calculations, the pseudo-radial distribution function  $\chi_{ij}$  for species  $i$  and  $j$  in the mixture must be evaluated. Kestin and Wakeham [16] proposed an equation for  $\chi_{ij}$  with the use of the density expansion equation for the radial distribution function of hard-sphere fluid mixtures. Since they used the density expansion equation truncated after the second-order density terms, the performance of the  $\chi_{ij}$  equation in the high-density region is unclear. To overcome this problem, we propose a new method to calculate the  $\chi_{ij}$  from the exact theoretical equation for the radial distribution functions of hard-sphere fluid mixtures proposed by Carnahan and Starling [17]. As shown by Vesovic and Wakeham [7], the pseudo-radial distribution function for pure gases,  $\chi_i$ , can be obtained from the pure-component viscosity by application of the hard-sphere expression for the viscosity of a pure gas [Eqs. (6) and (7) in Ref. 7]. We assume that the  $\chi_i$  is equal to the Carnahan–Starling radial distribution function of pure hard-sphere fluid  $i$  as follows:

$$\chi_i(\rho, T) = 1/(1 - \xi_3) + 1.5\xi_3^2/(1 - \xi_3)^2 + 0.5\xi_3^3/(1 - \xi_3)^3 \quad (6)$$

where  $\xi_3$  is the reduced density, defined by  $(1/6)\pi\rho N_{\text{AV}}d_i^3$ ,  $\rho$  is a molar density in  $\text{mol}\cdot\text{cm}^{-3}$ ,  $N_{\text{AV}}$  is Avogadro's number in  $\text{mol}^{-1}$ , and  $d_i$  is the hard-sphere diameter for species  $i$  in cm. Once the value of  $\chi_i$  is obtained from the pure-component viscosity data, the  $d_i$  can be determined from solving Eq. (6). Since a quadratic equation as for  $\xi_3$  is derived from Eq. (6) and the present experimental condition satisfied that only one real solution exists, the  $d_i$  value can be obtained analytically. Once the hard-sphere diameter for every constituent species in the mixture is determined from Eq. (6), the pseudo-radial distribution functions for species  $i$  and  $j$  in the mixture are obtained from the Carnahan–Starling radial distribution function of hard-sphere mixtures [17]. In the case of binary mixture of species  $i$  and  $j$ , the following equation is valid:

$$\begin{aligned} \chi_{ij}(\rho, T) = & 1/(1 - \xi_3) + 3(d_i d_j) \xi_2 / \{(d_i + d_j)(1 - \xi_3)^2\} \\ & + 2(d_i d_j)^2 \xi_3^2 / \{(d_i + d_j)^2 (1 - \xi_3)^3\} \end{aligned} \quad (7)$$

The reduced density  $\xi_k$  ( $k = 2, 3$ ) is defined as follows,

$$\xi_k = (1/6)\pi\rho N_{\text{AV}}(x_i d_i^k + x_j d_j^k) \quad (8)$$

where  $x_i$  is the mole fraction of species  $i$ . Since the Carnahan–Starling equation can give superior results for the thermophysical properties for



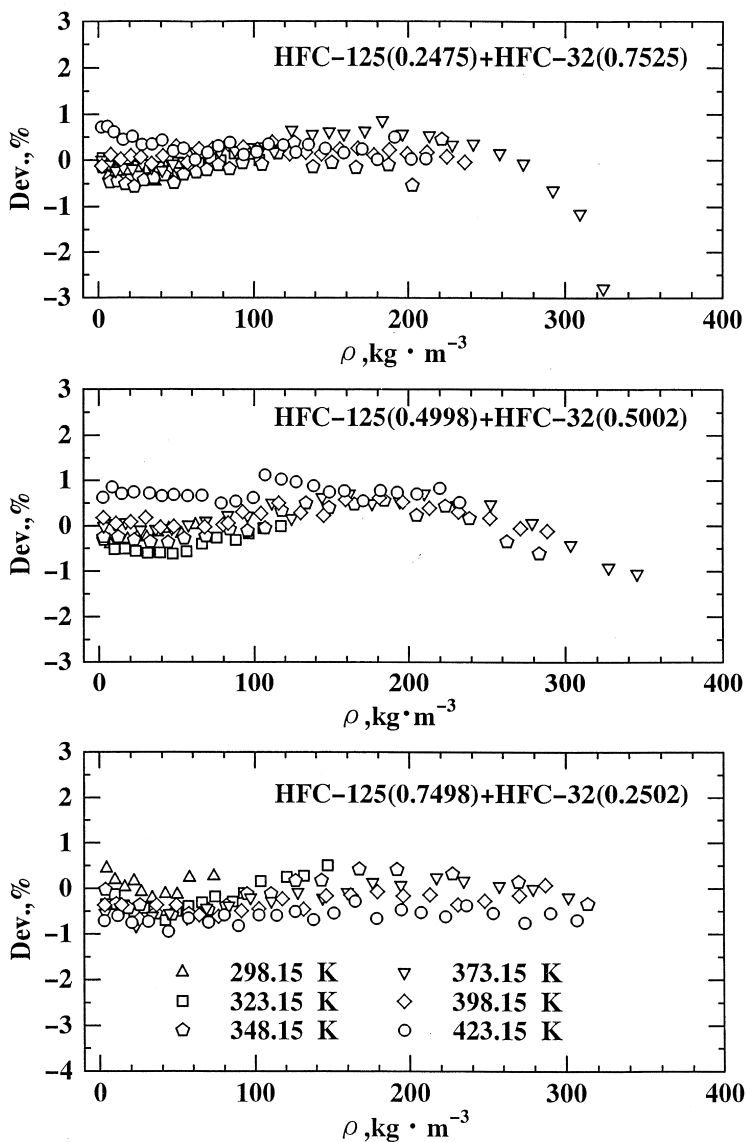


Fig. 4. Deviation plot of the present viscosity results from the values calculated by the V-W method with the mixing rule of Eqs. (6)–(8).  $\text{Dev.}(\%) = (\eta_{\text{exp}} - \eta_{\text{cal}}) / \eta_{\text{cal}} \times 100$ .

**Table IV.** Prediction Results of the V-W Method with Two Mixing Rules for HFC-125 + HFC-32 Mixtures

$x_{\text{HFC-125}}$	n.d. <sup>a</sup>	Original mixing rule for $\chi_{ij}$			Mixing rule of Eqs. (6)–(8)		
		Bias (%) <sup>b</sup>	AAD (%) <sup>c</sup>	Max. (%) <sup>d</sup>	Bias (%) <sup>b</sup>	AAD (%) <sup>c</sup>	Max. (%) <sup>d</sup>
0.7498	109	−0.28	0.37	0.94	−0.28	0.32	0.94
0.4998	114	0.16	0.40	1.2	0.16	0.40	1.0
0.2475	134	0.15	0.33	3.3	0.14	0.33	2.8

<sup>a</sup> Number of data.

<sup>b</sup> Bias (%) =  $\sum (\eta_{\text{exp}} - \eta_{\text{cal}}) / \eta_{\text{cal}} \times 100 / \text{n.d.}$

<sup>c</sup> AAD (%) =  $\sum |(\eta_{\text{exp}} - \eta_{\text{cal}})| / \eta_{\text{cal}} \times 100 / \text{n.d.}$

<sup>d</sup> Max. (%) = maximum of  $|(\eta_{\text{exp}} - \eta_{\text{cal}})| / \eta_{\text{cal}} \times 100.$

highly dense hard-sphere fluids, it is reasonable to consider that we can extrapolate the  $\chi_{ij}(\rho, T)$  to higher densities.

Figure 4 shows deviation plots of the experimental viscosity results and the calculated values from the V-W method with the proposed mixing rules. Comparisons between the calculated results from the V-W method with the original mixing rule for  $\chi_{ij}$  [7] and those with the mixing rule proposed in this study [Eqs. (6)–(8)] are listed in Table IV. It was found that the deviations of the three mixtures from the two mixing rules for  $\chi_{ij}(\rho, T)$  are almost the same. This suggests that the mixing rule for  $\chi_{ij}(\rho, T)$  proposed in this study is equivalent to the original mixing rule of Kestin and Wakeham [16] under the present experimental conditions. Furthermore, the prediction results for the binary mixtures show behavior quite similar to that for the correlation results with Eqs. (1)–(4) for pure HFCs. The ability of the V-W method to represent the density and temperature dependence of the viscosity for the HFC binary mixture may depend mainly on the viscosity correlations used for the pure constituent HFCs.

## 4. CONCLUSION

In this paper, we have reported the experimental results of the gaseous viscosity for the HFC-125 + HFC-32 system. The scaling parameters for the molecular interaction between HFC-125 and HFC-32 were determined with the extended corresponding-state theory and the viscosity data at 0.1 MPa. The viscosity values of the gaseous mixture under pressure were predicted with the modified Enskog theory developed by Vesovic and Wakeham. To extend the applicable density region for the modified Enskog theory, we

proposed a new method to calculate the pseudo-radial distributions based on the exact equation for the radial distribution function for hard-sphere fluids developed by Carnahan and Starling. From the comparison between the calculated results and the experimental viscosity values, both the proposed and the original methods give almost the same results under the present experimental conditions. We conclude that the Vesovic–Wakeham method should be a reliable method for viscosity calculations for mixtures of HFCs under pressure in the case where the viscosities both of pure HFCs under pressure and of gaseous HFC mixtures at 0.1 MPa can be correlated with a high accuracy.

## ACKNOWLEDGMENT

This work was funded by the Japan Space Utilization Promotion Center (JSUP), which is gratefully acknowledged.

## REFERENCES

1. M. Takahashi, N. Shibasaki-Kitakawa, C. Yokoyama, and S. Takahashi, *J. Chem. Eng. Data* **40**:900 (1995).
2. N. Shibasaki-Kitakawa, M. Takahashi, and C. Yokoyama, *Int. J. Thermophys.* **19**:1285 (1998).
3. M. Takahashi, N. Shibasaki-Kitakawa, and C. Yokoyama, *Int. J. Thermophys.* **20**:435 (1999).
4. M. Takahashi, N. Shibasaki-Kitakawa, and C. Yokoyama, *Int. J. Thermophys.* **20**:445 (1999).
5. C. Yokoyama, T. Nishino, and M. Takahashi, *Fluid Phase Equilibria.* **174**:231 (2000).
6. J. Kestin, K. Knierim, E. A. Mason, B. Najafi, S. T. Ro, and M. Waldman, *J. Phys. Chem. Ref. Data* **13**:229 (1984).
7. V. Vesovic and W.A. Wakeham, *Int. J. Thermophys.* **10**:125 (1989).
8. M. Takahashi, C. Yokoyama, and S. Takahashi, *J. Chem. Eng. Data* **33**:267 (1988).
9. M. Takahashi, C. Yokoyama, and S. Takahashi, *Trans. JAR* **6**:57 (1989).
10. C. Yokoyama, M. Takahashi, and S. Takahashi, *Int. J. Thermophys.* **15**:603 (1994).
11. K. Stephan, R. Krauss, and A. Laesecke, *J. Phys. Chem. Ref. Data* **16**:993 (1987).
12. R. T. Jacobsen and R. T. Stewart, *J. Phys. Chem. Ref. Data* **2**:757 (1973).
13. L. A. Weber, *Int. J. Thermophys.* **15**:461 (1994).
14. L. A. Weber and D. R. Defibaugh, *Int. J. Thermophys.* **15**:863 (1994).
15. H. Lee and G. Thodos, *Ind. Eng. Chem. Res.* **29**:1404 (1990).
16. J. Kestin and W. A. Wakeham, *Ber. Bunsenges. Phys. Chem.* **84**:762 (1980).
17. N. F. Carnahan and K. E. Starling, *J. Chem. Phys.* **51**:635 (1969).